Nonlinear Finite Element Analysis of Seismic Performance of Edge Slab-column Connections in R.C. Buildings

Prof. Dr. Abd El-Rahman Megahid Ahmed[1], Dr. Omar A. Farghal[1,] Dr. Abbas Mostafa[2], Eng. Mohamed Samier Sebaq[3]

[1]Civil Engineering Dept. Faculty of Engineering, Assuit University, Assuit, Egypt
[2]Civil Engineering Dept. Faculty of Engineering, Minia University, Minia, Egypt
[3]Housing and Building National Research Center, Giza, Egypt
Sebaq2020@yahoo.com

Abstract: R.C. flat-slab system is one of the most practical and commonly used structural systems in Egypt and many other countries. However, edge slab-column connections could pose a significant problem due to their brittle failure under punching mode around the perimeter of the column. Most codes provisions for the design of reinforced concrete flat-slabs are based on empirical formulations derived from experimental. The available test database consists of divergent types of slabs in some cases; it is limited due to the extensive cost and difficulty of a punching shear test to be carried out experimentally. Thus, there is a need for verification of the actual codes provisions, which can be simulated by finite element analysis (FEA). The FEA can replace accurately the experimental testing and can be used for parametric investigation, since they can indicate the effect of different aspects on punching shear failure, leading to possible recommendations for the design codes. In this paper, three-dimensional FEA of reinforced concrete edge slab-column connections are carried out using by ABAQUS Software [1], implementing the concrete damaged plasticity model is presented. The appropriate calibration of the connection model is performed in this study based on edge slab-column connections tests available. A parametric study on the seismic performance of edge slab-column connection using the key material and geometric parameters is performed in this investigation. The main parameters considered are column aspect ratio and steel slab reinforcement ratio. Generally, ACI 318-2014[2] and ECP203-2007[3] codes provisions appear to be conservative and underestimate the punching shear of flat-slabs.

[Abd El-Rahman Megahid Ahmed, Omar A. Farghal, Abbas Mostafa, Mohamed Samier Sebaq. **Nonlinear Finite Element Analysis of Seismic Performance of Edge Slab-column Connections in R.C. Buildings.** *N Y Sci J* 2017;10(4):9-18]. ISSN 1554-0200 (print); ISSN 2375-723X (online). http://www.sciencepub.net/newyork. 2. doi:10.7537/marsnys100417.02.

Keywords: Punching shear; Slab-column connections and Seismic performance.

1. Introduction

Flat-slab is one of the most common floor systems for large span residential and commercial buildings. The advantages of a flat-slab floor system are vast. It provides architectural flexibility, more clear space, less building height, easier formwork, and, consequently, shorter construction time and overall project economy.

Under lateral loads, many aspects of the behavior of edge slab-column connections in flat-slabs are uncertain. A serious problem that can arise herein is the brittle punching (two-way) shear failure due to poor transfer capacity of shearing forces and unbalanced moments between slabs and columns. In seismic zones, a structure can be subjected to strong ground motions, and, for economical design, a structure is considered to undergo deformations in inelastic range, therefore, in addition to strength requirement, slab-column connections must undergo these inelastic deformations without premature punching shear failure. In other words slab column connections must have adequate strength and ductility.

The punching shear behavior of edge slab-column connections under both gravity and lateral loads has been extensively investigated experimentally by several researchers (Durrani et al. [4]; Falamaki et al. [5]; Megally[11]; Regan et al. [17]; Hawkins et al. [18]; Choi et al. [13]; Kang et al. [19]). Most of the previous slab-column connection tests under lateral loads were conducted in the form of a component test using an isolated connection. This isolated connection was typically pin-supported at assumed inflection points of the slab.

Nonlinear finite element analyses (FEA) of reinforced concrete slabs can provide an insight into the slabs behavior; predict the possible modes of failure; support the experimental conclusions; and extend these conclusions to cases where the test measurements are not known/recorded. FEA of reinforced concrete slabs have been performed by many researchers (Menétrey (1994) [12]; Polak (2005) [16]; Negele at al. (2007) [15]; and Genikomsou and

Polak (2014) [6];studied reinforced concrete flat-slabs with two and three dimensional models using solid, shell elements for concrete and truss element for reinforcement steel.

This research study presents on numerical FE models developed to predict the behavior of edge slab-column connections under gravity and cyclic lateral loads. Three-dimensional nonlinear FE models have been developed in order to simulate the behavior of the edge slab-column connections, which aiming at studying the lateral load-drift ratio response, shear stress response and the crack pattern. The purpose of the present study is to quantify the effect of column aspect ratio and slab longitudinal reinforcement ratio on the behavior of slab-column connections by using finite element analysis platform (ABAQUS).

2. Finite Element Modelling

2.1Concrete Damage Plasticity Model

The concrete damage plasticity model is a continuum, plasticity-based, damage model, which assumes two main failure mechanisms: the compressive crushing and the tensile cracking concrete. The concrete in compression can be modeled with the Hognestad and Lee et al. [8:10] and the concrete in tension can be modeled using Nayal and Rasheed (2006) [14]. Prior to conducting numerical analysis of edge slab-column connections some input data for failure criteria in ABAQUS developed by Kupfer et al. [9] with five parameters are taken into account.

3. Simulation and Calibration of Edge Slab-Column Connections

In order to calibrate the required parameters, especially the dilation angle and viscosity parameter in the employed material models of concrete and steel in ABAQUS, the numerical simulations are validated against experimental studies of two edge slab-column connections subjected to gravity and cyclic lateral loading. In this section, two exterior connections are selected from previous experimental tests [4:9] to be simulated using ABAQUS. In order to best correlate ABAQUS predictions with experimental results, the simulations presented later are based on adjusted values for the dilation angle in numerical models by trial and error within the range of 30° to 40°. The details of the incorporated specimens in terms of geometric dimension, boundary condition, loading condition (gravity load or lateral load) and material properties of both concrete and steel reinforcement are given and the numerical models meshed by 3D solid element for concrete and truss element for steel reinforcement.

3.1. Edge Slab-Column Connections Modelling of Durrani et al. (1995) and Megally (2000)

Edge slab-column connections (IE), (MG-7) tested by Durrani et al. (1995) [4] and Megally (2000) [11] respectively, are taken as reference specimens for numerical modeling as shown in Fig.1 and Fig.2. The parameters of the test slabs corresponding to the FE model and the summary of the material properties used in the FE modeling are shown in Table 1 and 2.

The edge slab-column connection is preloaded with uniaxial lateral load in the direction (perpendicular to the free slab edge) is increased until slab-column connection failure. The gravity shear ratio of edge slab-column connections IE and MG-7 tested by Durrani and Megally, V_g/V_n are 0.1 and 0.29 respectively. The term V_g is the shear force transferred at the slab-column connection due to gravity loads and is calculated using tributary area, while V_n is the punching shear strength of the connection in the absence of moment transfer. Cyclic lateral loading procedures are displacement based and the drift ratio parameter is used. Drift ratio is defined as the relative displacement between the top and bottom of the column divided by the column height.

Table 1: Details of slab model specimen dimensions

Connection type	Durrani(IE)	Megally (MG-7)
Slab dimensions (mm)	2000x1570x115	1900x1350x150
Column dimensions(mm)	250x250	250x250
Slab thickness h (mm)	115	150

Table 2: Material properties used in edge slab-column connection

Connection type	Durrani (IE)	Megally (MG-7)
Concrete modulus of elasticity E_c, MPa	22005.1	26600
Concrete cylinder compressive strength f_c', MPa	20.7	31.0
Steel yield strength of slab and column f_y, MPa	379	415

3.2. Numerical Results

These edge slab-column connections IE and MG-7 were tested under gravity load and horizontal reversed cyclic displacements by Durrani et al. and Megally. The response of the specimens is described by means of horizontal cyclic load and drift response. The hysteretic loops in the specimen exhibited pinching, denoting strength and stiffness degradation. In contrast, when the cyclic loading analysis was performed in ABAQUS, the hysteretic loops obtained from the analyses did not exhibit the pinching effect.

It must be mentioned that the complexity in constitutive modeling of concrete and the adoption of perfect bond between concrete and reinforcement, created problems in the hysteretic simulations in ABAQUS. Alternatively, in this research, cyclic loading analysis is presented and the results of the FE simulations show good agreement compared to the experimental results as shown in Fig.3 and Fig.4. Simulations of test specimens show brittle failure after obtaining peak lateral load similar to the test peak loads. Table 3 compares the experimental and numerical results in terms of shear stress capacity, peak lateral load and drift ratio at the peak load. Yielding of the flexural reinforcement took place during the FEA, the tension reinforcement (top and bottom) at the face of the column in the direction of the cyclic loading yielded at drift ratio 1.0% to 2.0%. It is observed from lateral load-drift ratio curve of this slab shown in Fig.5 and Fig.6 that there are also some difference in the lateral load-drift ratio behavior between present FE analysis and experimental results (EXPT). It is observed that for edge slab-column connections, the maximum lateral load obtained numerically (11.65 kN, 54.17 kN) respectively, are higher than the experimental test ones (10.13 kN, 48.38 kN), respectively, which represents 15% and 11.96% FE overestimating.

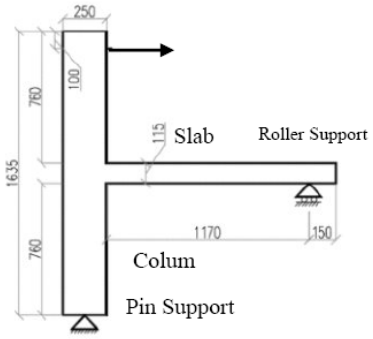

Fig. 1: Schematic diagram of edge slab-column connection IE by Durrani et al. (1995).

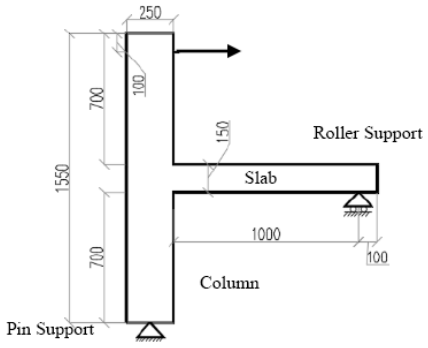

Fig. 2: Schematic diagram of edge slab-column connection MG-7 by Megally (2000).

Table 3: Comparison of Test and FEA results

Results		Connection (IE)		Connection (MG-7)	
		Test Results	FEA Results	Test Results	FEA Results
Punching Shear stress, MPa		1.42	1.68	2.71	3.39
Peak lateral load, kN	+ve	10.13	11.65	48.38	54.17
	-ve	-9.47	-11.41	-34.19	-42.46
Drift at peak load, %		2.00	2.50	2.00	1.50

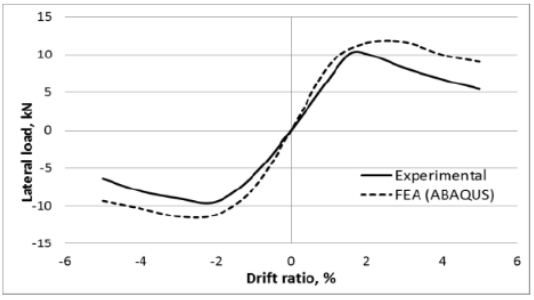

Fig. 3: Comparative lateral load-drift ratio backbone curves for edge slab-column connection (IE) by Durrani et al. (1995).

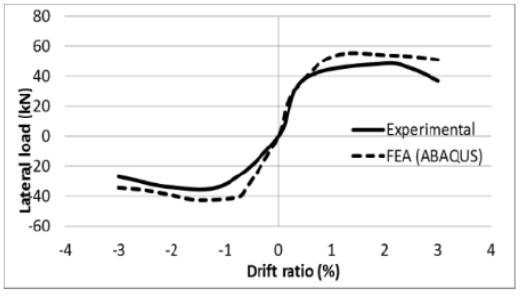

Fig. 4: Comparative lateral load-drift ratio backbone curves for edge slab-column connection (MG-7) by Megally (2000).

4. Numerical Modelling Approach and Variables

The prototype for the flat-slab specimens was selected as a single edge slab-column connection 6.0 x 6.0 m and a slab thickness of 200 mm, resulting in a slab span-thickness ratio of 30. The prototype and the numerical model specimens were designed according to modern codes (ACI318-14). The prototype structure was scaled down to approximately two-third

for the modeled specimens that were a 2.3 x 2.3 m in slab dimension and a slab thickness of 135 mm. The long span direction, which is horizontal in the plan view and side view in Fig.5, is referred to as longitudinal direction hereafter, while the short span direction is referred to as transverse direction. The modeling of specimens was designed to show the effect of aspect ratio of column section and the slab steel reinforcement ratio in the connection region on the seismic performance of edge slab column connections. The edge slab-column connections of flat-slab buildings were modeled under combined gravity and cyclic lateral load.

In particular, the numerical model aims to investigate the effect of column aspect ratio and slab flexural reinforcement, on the punching shear capacity of flat-slabs under gravity and lateral loads. The numerical model includes 8 edge slab-column connection specimens divided into two groups. The first group (A) includes five specimens, SAR-1, SAR-1.5, SAR-2.25, SAR-3 and SAR-4 to study the effect of column aspect ratio. Fig.6a shows the layout of top and bottom reinforcement meshes of the slab. Details of the group (A) reported and summarized in Table 4. The five specimens have the same of slab geometry, reinforcement ratio and material properties. The main difference between specimens was the column aspect ratio which varied as indicated in Table 4.

The second group (B) includes four specimens, SRR1, SRR2, SRR3 and SRR4 to study the effect of slab flexural reinforcement ratio, on seismic behavior of slab-column connections. Figures 6a to 6d show the layout of top and bottom slab reinforcement meshes for group (B) specimens. Details of these specimens are summarized in Table 5. The four specimens have the same slab geometry and column dimensions (300x300 mm). The amount of slab flexural reinforcement in group (B) was relatively high to avoid flexure failure of slabs prior to punching shear failure. There is a current trend to concentrate slab flexural reinforcement in the column vicinity. The current American Building Code ACI318-14 requires that reinforcement running perpendicular to the slab free edge, sufficient to resist the total negative and positive moments resulting from lateral loading at exterior columns, be placed in the column vicinity within a strip width c_2+3h, where c_2 the column dimension parallel to the slab free edge and h is the slab thickness. Moreover, Grossman (1997) [7] recommends that flat slab-column framing should contribute in resisting lateral forces, in this case the slab flexural reinforcement in the column vicinity must be increased to resist the significant unbalanced moment transferred between slab and column. Thus, it seems that the relatively high flexural reinforcement ratio used in the specimens of this series is just sufficient to represent this practice. The lateral displacement protocol used in this numerical program was derived from a lateral routine developed FEMA 356 (2000) [20] and is depicted in Fig.7.

5. ACI 318-2014 and ECP203-2007 Codes Provisions

The flat-slab provisions in ACI318-2014 and ECP203-2007 codes are based on the assumption that the punching shear failure surface will develop at an angle of 45 degree. The permissible nominal shear stresses in the concrete are empirically derived based on a critical section located at half the effective depth of the slab away from the perimeter of the load.

ACI 318-14 requires that v_c, the shear stress at slab-column connection calculated not exceed the smallest of the following expressions in (MPa):

$$v_c = \frac{1}{3}\sqrt{f'_c} \quad (1) \qquad v_c = \left[1 + \frac{2}{\beta_c}\right]\frac{\sqrt{f'_c}}{6} \quad (2) \qquad v_c = \left[2.0 + \frac{\alpha_s d}{b_0}\right]\frac{\sqrt{f'_c}}{6} \quad (3)$$

Where, v_c, the nominal shear capacity of the concrete, β, is the ratio of the longer side to the shorter side of the column, α_s is 40 for interior column, 30 for edge columns, and 20 for corner columns, b_o is the length of critical shear perimeter taken at a distance of 0.5d away from the column face and f'_c is the concrete cylinder compressive strength.

The Egyptian code states that the smallest of the following three values represents the concrete punching shear strength q_{cup} in (MPa).

$$q_{cup} = 0.316\left[0.5 + \frac{a}{b}\right]\sqrt{\frac{f_{cu}}{1.5}} \quad (4) \qquad q_{cup} = 0.8\left[0.2 + \frac{\alpha . d}{b_0}\right]\frac{\sqrt{f_{cu}}}{6} \quad (5) \qquad q_{cup} = 0.316\sqrt{\frac{f_{cu}}{1.5}} \quad (6)$$

Where, q_{cup}, the nominal shear capacity of the concrete, a, is the column dimension in the analysis direction, b, is the column dimension in the perpendicular direction, α is 4 for interior column, 3for edge columns, and 2 for corner columns,

b_o is the length of critical shear perimeter taken at a distance of 0.5d away from the column face and f_{cu} is the concrete cubic compressive strength.

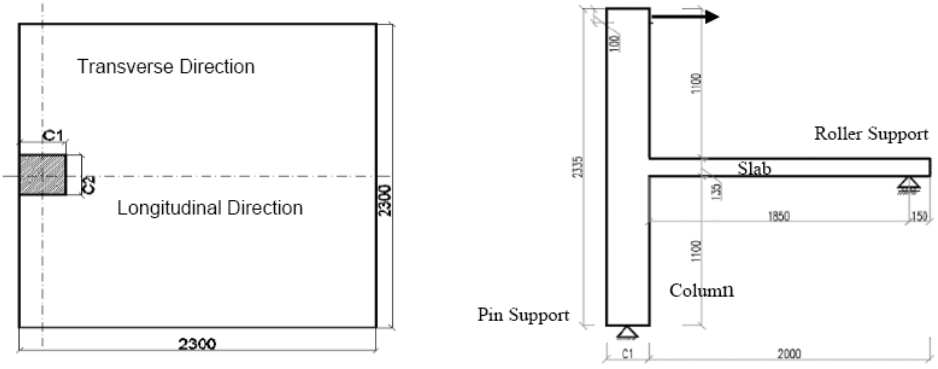

Fig. 5: Typical numerical model of connection specimen (plan view and elevation).

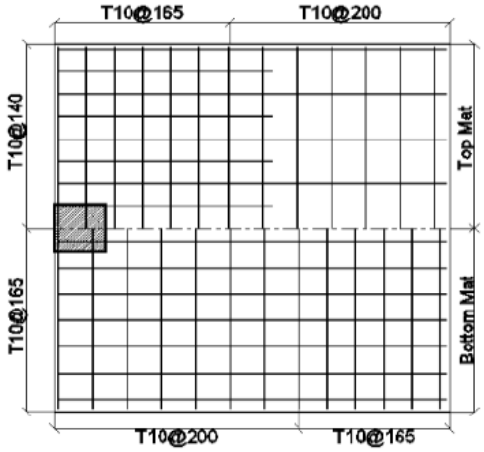

Fig. 6a: Layout of slab reinforcement for all specimens expect SRR2,SRR3 and SRR4.

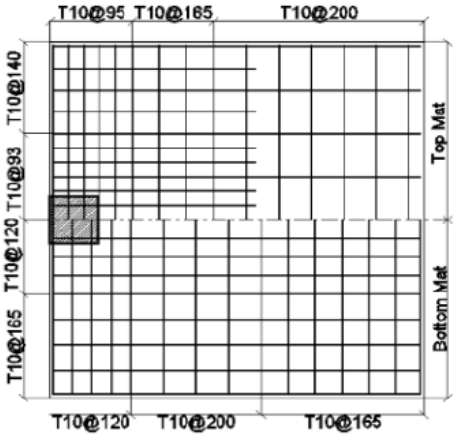

Fig. 6b: Layout of slab reinforcement for specimen SRR2.

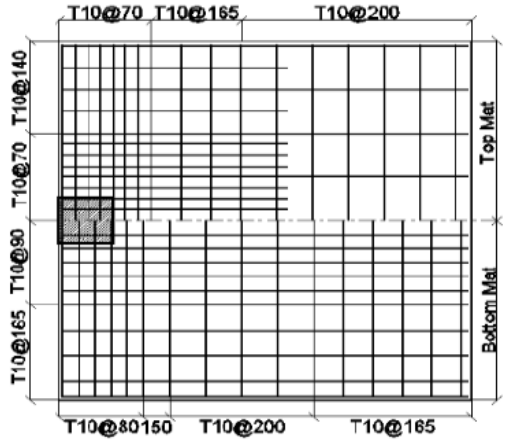

Fig. 6c: Layout of slab reinforcement for specimen SRR3.

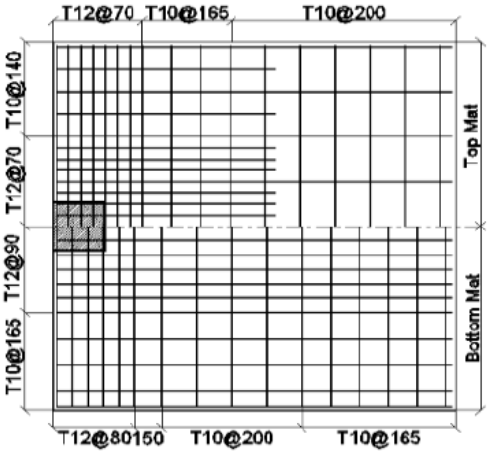

Fig. 6d: Layout of slab reinforcement for specimen SRR4.

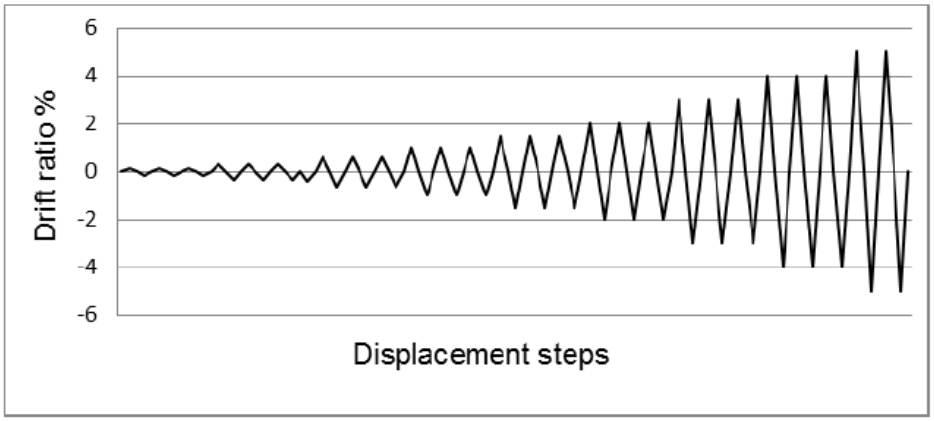

Fig. 7: Lateral displacement routine

Table 4: Specimens details

Specimen ID.	Column Dimensions		Slab Thickness h (mm)	Concrete Cylinder Strength f'_c ,Mpa	Steel Yield Strength f_y ,MPa	Top Reinforcement Ratio %		Bottom Reinforcement Ratio %	
	C_1 (mm)	C_2 (mm)				c_2+3h	Full width	c_2+3h	Full width
First Group (A)									
SAR-1	300	300	135	20	400	0.53	0.55	0.42	0.45
SAR-1.5	360	250	135	20	400	0.62	0.55	0.49	0.45
SAR-2.25	450	200	135	20	400	0.62	0.55	0.49	0.45
SAR-3	520	175	135	20	400	0.62	0.55	0.49	0.45
SAR-4	600	150	135	20	400	0.67	0.55	0.54	0.45
Second Group (B)									
SRR1	300	300	135	20	400	0.54	0.55	0.42	0.45
SRR2	300	300	135	20	400	0.84	0.68	0.53	0.52
SRR3	300	300	135	20	400	1.15	0.81	0.74	0.68
SRR4	300	300	135	20	400	1.66	1.03	1.07	0.84

6. Punching Shear Strength Parametric Study Results

6.1. Effect of Column Aspect Ratio

Column aspect ratios of edge slab-column connection specimens varying from 1.0 to 4.0 with fixed cylinder compressive strength 20MPa were analyzed. The purpose of this section is to evaluate an effect of column aspect ratio ($\beta c = c_1/c_2$ = side length ratio of column section in the direction of lateral loading (c_1) to the direction perpendicular to lateral loading (c_2) on the punching shear strength under gravity and lateral loading. The FEA results for each specimen are described in Table 5. In numerical results the tensile reinforcement yielded first at the column face, the cracking propagation in all specimens started on the tension side of the slabs. The cracks started from the inner corners of the columns and developed towards the edges of the slabs. Under lateral loads, the lateral load-drift ratio backbone curves of specimens with column aspect ratio varying from 1.0 to 4.0 are given in Fig.8. It is seen that with increasing of column aspect ratio the lateral load increases. However, this is not exactly true for punching shear stresses. The analytical results (Present FE analysis) getting from parametric study (column aspect ratio βc) specimens) are compared with predicted nominal shear values based on punching shear capacity according to ACI 318-14 and ECP203-2007 codes for flat-slabs in Table 5. It is observed from the Table 5 that in most of the cases ACI 318-14 and ECP203-2007 codes predictions are conservative; giving underestimated shear strength of edge slab-column connections. The shear strength of slab-column connection is decrease with the increase of column aspect ratio beyond 1.5 according to ACI 318-14 and ECP203-2007 codes.

In order to compare FEA results presented with previous experimental results, a tested database under gravity and lateral loading of reinforced concrete flat slabs was used. This database of previous tests has results of two-way slabs supported on rectangular columns presented by Hawkins et al. (1974) [18], Falamaki et al. (1977) [5], Regan at al. (1985) [17], and Choi et al. (2007) [13].

From numerical FEA results and previous experimental data in Fig.9, when column aspect ratio increases, shear strength increases until column aspect ratio of 2.0 to 2.25. Beyond column aspect ratio of 2.25, the shear strength decrease with increasing column aspect ratio. Two vertical dash lines in Fig.9 indicate limits after which punching capacity decreases with increasing column aspect ratio. This confirms that the punching shear provisions of ACI318-2014 and ECP203-2007 codes provisions underestimate the average shear stress of edge slab-column connections subjected to gravity and lateral loading. Fig.10 shows in sequence the contour plots of the minimum principal plastic strain at the integration points and, predicted crack patterns for specimens (SAR-1, SAR-1.5, SAR-2.25, SAR-3 and SAR-4).

Table 5: Specimens (SAR-1, SAR-1.5, SAR-2.25, SAR-3 and SAR-4) results summary.

Specimen/Results	SAR-1	SAR-1.5	SAR-2.25	SAR-3	SAR-4
Maximum positive lateral load, kN	18.44	21.11	24.66	28.77	37.41
Maximum negative lateral load, kN	-12.82	-15.01	-18.10	-20.85	-26.92
Maximum positive unbalanced moment, kN.m	36.88	42.22	49.32	57.54	74.82
Maximum negative unbalanced moment, kN.m	-25.64	-30.02	-36.20	-41.7	-53.84
Shear stress capacity vu, MPa	2.80	2.99	3.59	2.87	2.43
Nominal concrete shear stress capacity according to ACI318-2014,MPa	1.49	1.49	1.41	1.24	1.19
Nominal concrete shear stress capacity according to ECP203-2007,MPa	1.29	1.29	1.22	1.079	0.968

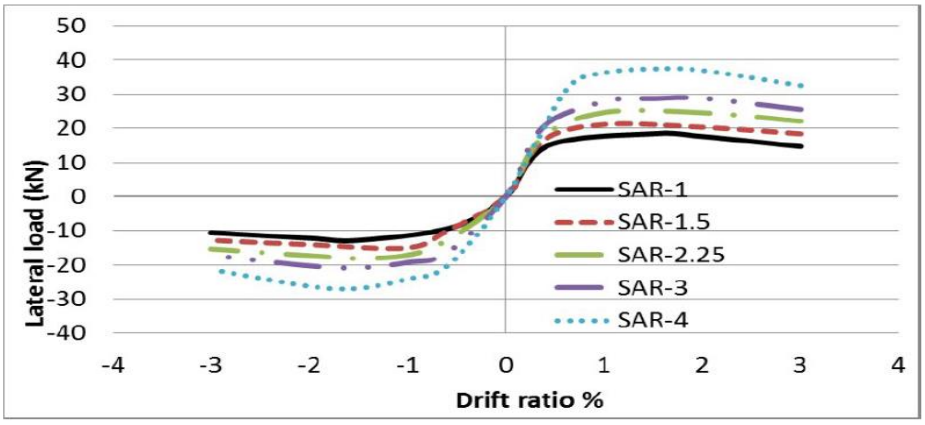

Fig. 8: Load-drift ratio cyclic backbone responses for specimens with varying column aspect ratio.

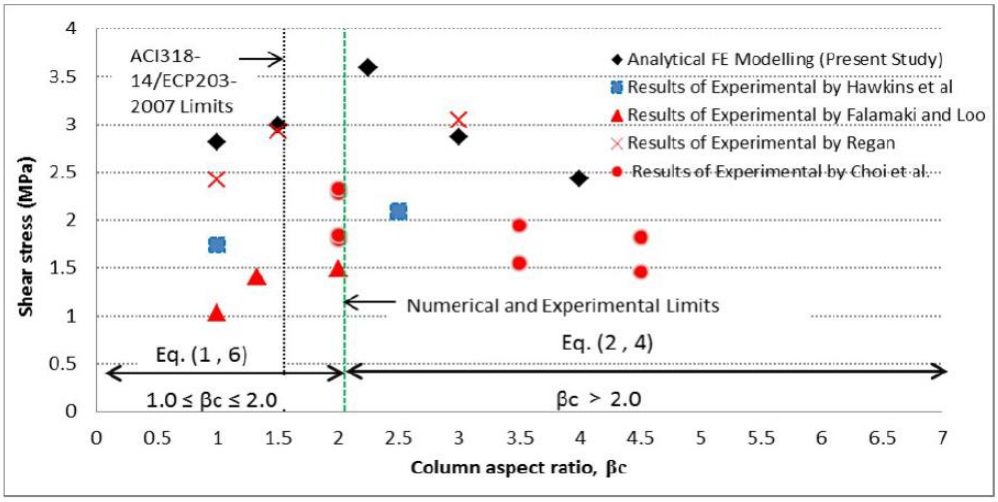

Fig. 9: Comparisons of punching shear stress from analytical FE results (present study) and previous experimental data with ACI318-14 and ECP203-2007 codes provisions limits for varying column aspect ratio specimens.

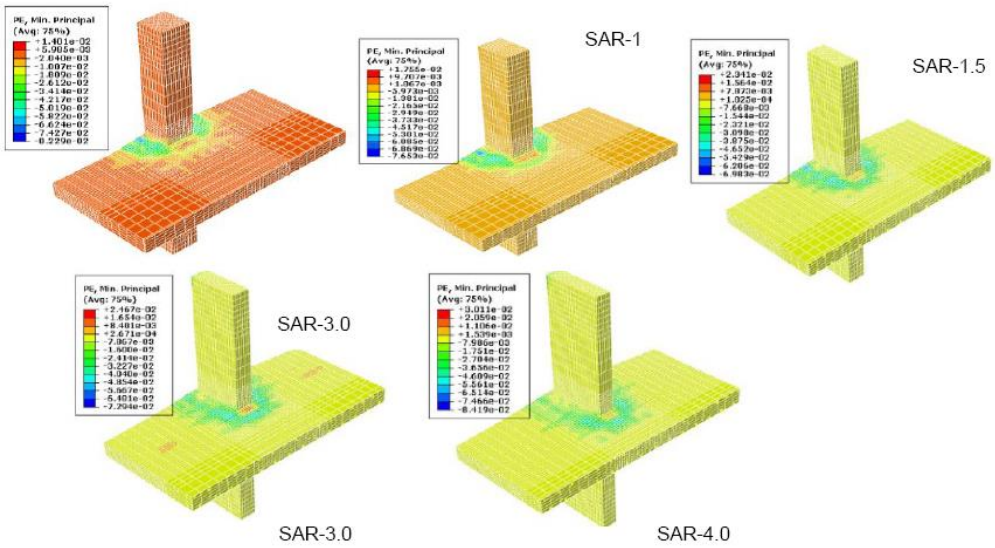

Fig. 10: Predicted crack pattern for the specimens (SAR-1, SAR-1.5, SAR-2.25, SAR-3 and SAR-4).

6.2. Effect of Slab Reinforcement Ratio

This section presents a comparison between edge slab-column connection specimens with varying slab flexural reinforcement ratio in the direction of lateral load and with fixed cylinder compressive strength 20 MPa and column aspect ratio of 1. The top tensile reinforcement ratio of specimens (SRR1, SRR2, SRR3 and SRR4) in the transfer width (c_2+3h) are 0.53%, 0.75%, 1.17%, and 1.68% respectively. The FEA results for each specimen are described in Table 6. Under lateral loading the load-drift ratio cyclic backbone curves of specimens with varying reinforcement ratio are given in Fig.11. It is seen that with increasing slab reinforcement ratio the lateral load and lateral drift capacity increase due to increased flexural capacity. Slab-column connections with higher percentage of reinforcement have failed in punching shear. Thus, lateral load is increased significantly by increasing percentage of flexural reinforcement. Table 6 compares the predictions of analytical results (present FE analysis) with the ACI code (ACI 318-2014) and ECP code (ECP203-2007) expressions to investigate the influence of flexural reinforcement ratio. ACI and ECP codes have totally ignored the effect of flexural reinforcement in calculating punching shear capacity. From Table 6 it is clear that with increasing the percentage of reinforcement, the value of the punching shear capacity is increased. The change in behavior of slab-column connections with the change in the reinforcement ratio was particularly noticeable for higher values of slab reinforcement ratio. It can be observed that after a similar initial elastic response, the behavior of the slab-column connections varies tremendously depending on the percentage of reinforcement. The shear stress capacity enhancement is 44.3%, 88.2% and 125% for reinforcement ratios 0.75%, 1.17% and 1.68% respectively under fixed concrete compressive strength 20MPa. Fig.12 shows in sequence the contour plots of the minimum principal plastic strain at the integration points and predicted crack patterns for specimens (SRR1, SAR2, SAR3 and SAR4).

Table 6: Specimens (SRR1, SRR2, SRR3 and SRR4) results

Specimen/Results	SRR1	SRR2	SRR3	SRR4
Maximum positive lateral load, kN	18.44	23.34	31.05	35.72
Maximum negative lateral load, kN	-12.82	-17.30	-23.80	-28.88
Maximum positive unbalanced moment, kN.m	36.88	46.68	62.10	75.36
Maximum negative unbalanced moment, kN.m	-25.64	-34.60	-47.60	-57.76
Shear stress capacity v_u, MPa	2.80	4.04	5.27	6.31
Nominal concrete shear stress capacity according to ACI318-2014,MPa	1.49	1.49	1.49	1.49
Nominal concrete shear stress capacity according to ECP203-2007,MPa	1.29	1.29	1.29	1.29

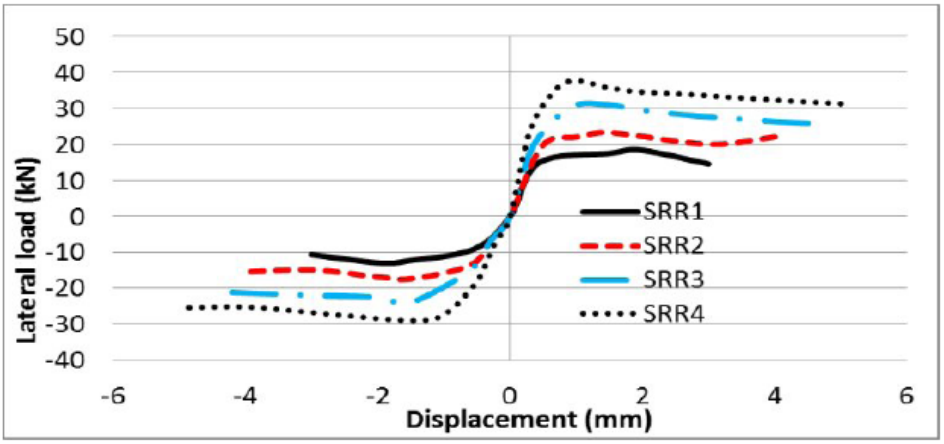

Fig. 11: Load-drift ratio cyclic backbone curves for specimens with varying slab reinforcement ratio.

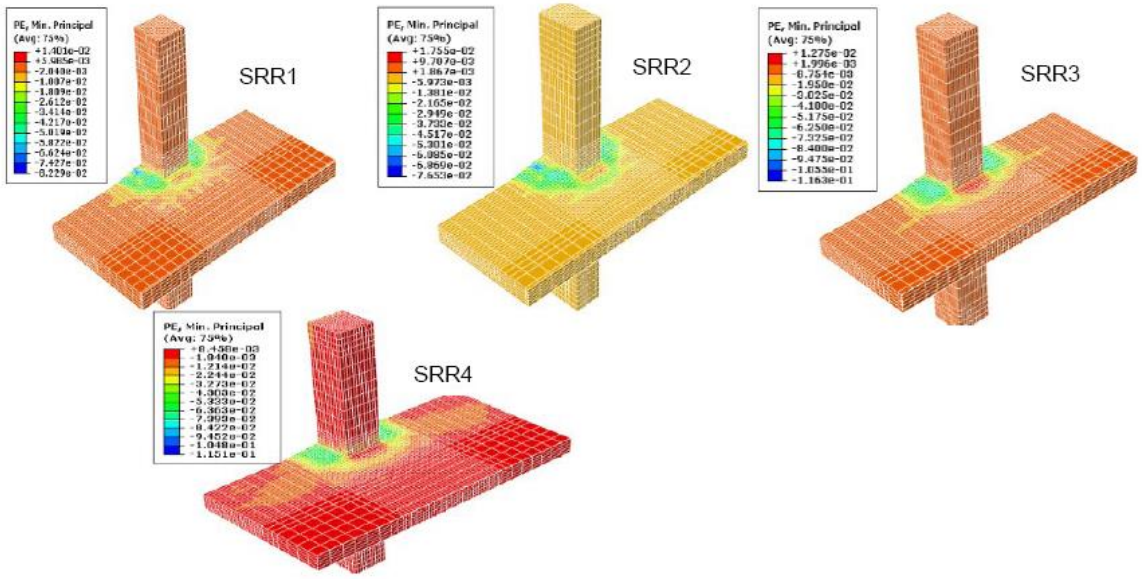

Fig. 12: Predicted crack pattern for the specimens (SRR1, SRR2, SRR3 and SRR4).

8. Conclusions

Numerical modeling of edge slab-column connections with emphasis on punching shear behavior of reinforced concrete flat-slabs by using 'ABAQUS' FEA platform based on nonlinear finite element method has been performed successfully and the numerical results have shown a good correlation with available experimental and numerical results.

The following conclusions based on the results of this work can be drawn:

1- Finite element results show slightly higher stiffness than the experimental results. This may be due to non-availability of some data used in the FE modeling such as experimental test setup. Moreover, the effects of concrete micro cracking*, bond slip (between concrete and reinforcement), dowel action and aggregate interlock were absent in the finite element modeling.

2- Flexural reinforcement ratio has an important effect on seismic punching shear strength of R.C. edge flat slab-column connections. Punching capacity increases with the increase of the of flexural reinforcement ratio.

3- The change of square column size to rectangular column with the same area (changing column aspect ratio), where the long side is perpendicular to the slab edge have increased the punching shear strength until column aspect ratio of 2.25 while increasing column aspect ratio

beyond 2.25 decreased the punching shear strength decreased.

4- ACI 318-14 and ECP203-2007 code formulas for punching shear strength have been found to be conservative.

References

1. Abaqus Theory Manual (Volume-I-V), "Version 6.14", Simulia, USA.
2. ACI 318 (2014), "Building Code Requirements for Structural Concrete", American Concrete Institute, Farmington Hills, MI, USA.
3. ECP203 (2007), "Egyptian Code for Concrete Structures", Housing and Building National Research Cente, Cairo, Egypt.
4. Durrani, A. J., Du, Y., and Luo, Y. H. 1995. "Seismic Resistance of Non-ductile Slab Column Connections in Existing Flat-Slab Buildings," ACI Structural Journal, v. 92, No.4, pp. 479-487.
5. Falamaki M., Loo Y.C. (1992)"Punching Shear Tests of Half-Scale Reinforced Concrete Flat Plate Models with Spandrel Beams", ACI Structural Journal, 89(3), May–June, 263–271.
6. Genikomsou, A.S., and Polak, M.A. (2014) "Finite Element Analysis of Punching Shear in Flat Slabs using ABAQUS", Structures Congress 2014, SEI of ASCE, April 3-5, 2014, Boston, Massachusetts, USA.
7. Grossman, J.S (1997). Verification of Proposed Design Methodologies for Effective Width of Slabs in Slab-Column Frames. ACI Structural Journal, V. 94, No. 2, March-April, pp. 181-196.
8. Hognested E. Study of Combined Bending and Axial in Reinforced Concrete Members.1951.
9. Kupfer, H., Hilsdorf, H.K., and Rusch, H. (1969). "Behahior or concrete under biaxial stresses." ACI J, 66(8):656-666.
10. Lee, J., and Fenves, G.L. (1998). "A plastic-damage concrete model for earthquake analysis of dams." Earthquake eng and struct dyn,27(9):937-56.
11. Megally, S. (2000). Punching Shear Resistance of Concrete Slabs to Gravity and Earthquake Forces. Ph.D. Dissertation, Department of Civil Engineering, the University of Calgary, Calgary, Alberta, Canada, 266pp.
12. Menetrey, P., Walther, R., Zimmermann, T., William, K., and Regan, P.,"Simulation of Punching Failure in Reinforced-Concrete Structures", ASCE - Journal of Structural Engineering, Vol. 123, No. 5,1997, pp. 652-659.
13. M. S. Choi, J. M. Ahn, K. S. Lee, and S. W. Shin, "Influence of Column Aspect Ratio on the Punching Shear Strength of Flat Plate Slab-Column Connections," Journal of Architectural Institute of Korea (Structure & Construction), Vol.21, No. 10, 2005, pp. 79-86 (in Korean).
14. Nayal, R. and Rasheed, H.A. (2006). "Tension stiffening model for concrete beams reinforced with steel and FRP bars", Journal of Materials in Civil Engineering, Vol. 18, No.6, pp. 831–841.
15. Negele, A., Eligehausen, R., Ožbolt, J., and Polak, M.A. (2007). "Finite-element simulations on punching tests of shear retrofitted slab-column connections." Proc., IA-FraMCoS-6: International Association of Fracture Mechanics for Concrete and Concrete Structures, Catania, Italy, 911–918.
16. Polak, M. A. (2005). "Shell finite element analysis of RC plates supported on columns for punching shear and flexure." International J. for Comp.-Aided Eng. and Software, 22(4):409-428.
17. Regan, P. E., and Braestrup, M. W. 1985. "Punching Shear in Reinforced Concrete," Bulletin D'Information No. 168, Comité Euro-International du Béton, 1985.
18. Hawkins, N. M., Mitchell, D., and Sheu, M. S. 1974. "Cyclic Behavior of Six Reinforced Concrete Slab-Column Specimens Transferring Moment and Shear," Progressive Report 1973-1974, NSF Project GI 38717, Section II, Department of Civil Engineering, University of Washington, Seattle, 50 pp.
19. Rha. C, Kang, T. H-K, Shin. M, Yoon. J.B "Gravity and Lateral Load-Carrying Capacities of Reinforced Concrete Flat Plate Systems," ACI Structural Journal, V. 111, No. 4, July-Auguest 2014., pp. 193-203.
20. Federal Emergency Management Agency (FEMA) 356 (2000). Prestandard and commentary for the seismic rehabilitation of buildings, Washington, D.C.

3/15/2017